



Deficiency in interferon type 1 receptor improves definitive erythropoiesis in *Klf1* null mice

Maria Francesca Manchinu¹ · Carla Brancia² · Cristian Antonio Caria¹ · Ester Musu¹ · Susanna Porcu¹ · Michela Simbula¹ · Isadora Asunis¹ · Lucia Perseu¹ · Maria Serafina Ristaldi¹

Received: 21 April 2017 / Revised: 21 September 2017 / Accepted: 29 September 2017 / Published online: 11 December 2017
© The Author(s) 2017. This article is published with open access

Abstract

A key regulatory gene in definitive erythropoiesis is the transcription factor Krüppel-like factor 1 (*Klf1*). *Klf1* null mice die in utero by day 15.5 (E15.5) due to impaired definitive erythropoiesis and severe anemia. Definitive erythropoiesis takes place in erythroblastic islands in mammals. Erythroblastic islands are formed by a central macrophage (Central Macrophage of Erythroblastic Island, CMEI) surrounded by maturing erythroblasts. *Interferon-β* (*IFN-β*) is activated in the fetal liver's CMEI of *Klf1* null mice. The inhibitory effect of *IFN-β* on erythropoiesis is known and, therefore, we speculated that *IFN-β* could have contributed to the impairment of definitive erythropoiesis in *Klf1* knockout (KO) mice fetal liver. To validate this hypothesis, in this work we determined whether the inactivation of type I interferon receptor (*Ifnar1*) would ameliorate the phenotype of *Klf1* KO mice by improving the lethal anemia. Our results show a prolonged survival of *Klf1/Ifnar1* double KO embryos, with an improvement of the definitive erythropoiesis and erythroblast enucleation, together with a longer lifespan of CMEI in the fetal liver and also a restoration of the apoptotic program. Our data indicate that the cytotoxic effect of *IFN-β* activation in CMEI contribute to the impairment of definitive erythropoiesis associated with *Klf1* deprivation.

Introduction

Klf1 is essential for definitive erythropoiesis in mice [1, 2] and man [3] and is a key regulator of many erythroid genes [4, 5]. *Klf1* KO mice are strongly anemic and die by E15.5 [1, 2]. Early reports indicated that progenitor cells fail to undergo terminal erythroid differentiation in *Klf1*^{-/-} embryos and latter stage erythropoiesis is compromised [6, 7]. We previously described a non-erythroid specific target of *Klf1*, the endonuclease enzyme DNaseII-alpha of CMEI

[8]. Definitive erythropoiesis takes place in erythroblastic islands in mammals. Erythroblastic islands are highly specialized hematopoietic tissue sub-compartments that play a critical role in regulating erythropoiesis. Erythroblastic islands contain a CMEI surrounded by erythroid cells at different stage of maturation [9–12]. The central macrophage plays several roles in erythroid maturation including the engulfment of extruded nuclei from erythroblasts and degradation of the nuclear DNA by DNase II-alpha. *Dnase2a* KO mice have a peculiar erythroid phenotype. The mice die around E17.5 of lethal anemia, which is caused by *IFN-β* production by CMEIs, which contain a large amount of undigested DNA [13]. *IFN-β* produced in the fetal liver inhibits the erythropoiesis that occurs in association with macrophages at the erythroblastic island. Undigested DNA directly stimulates CMEIs to express *IFN-β* and, consequently, interferon-responsive genes, which inhibit erythropoiesis by apoptosis and kill the embryos [13–16].

Similarly, we have previously shown that *IFN-β* is activated in the fetal liver of *Klf1* KO embryos [8]. This observation suggested to us that *IFN-β* could have contributed to the *Klf1* KO phenotype, exacerbating the defect in definitive erythropoiesis.

Edited by R De Maria

Electronic supplementary material The online version of this article (<https://doi.org/10.1038/s41418-017-0003-5>) contains supplementary material, which is available to authorized users.

✉ MariaSerafina Ristaldi
ristaldi@irgb.cnr.it

¹ Istituto di Ricerca Genetica e Biomedica del Consiglio Nazionale delle Ricerche (IRGB-CNR), Cittadella Universitaria, SS 554 bivio per Sestu Km 4,5, 09042 Monserrato, Cagliari, Italy

² Dipartimento di Scienze Biomediche. Facoltà di Medicina e Chirurgia, Cittadella Universitaria, SS 554 bivio per Sestu Km 4,5, 09042 Monserrato, Cagliari, Italy

We determined whether the inactivation of *Ifnar1* would ameliorate the phenotype of *Klf1* KO mice by improving the lethal anemia. Here, we show that *Klf1/Ifnar1* double KO embryos survive longer in utero. The longer lifespan is accompanied by an improvement of definitive erythropoiesis. Erythrocytes undergo terminal erythroid differentiation and enucleate more efficiently, although with a reduced efficiency compared to WT mice. The amelioration of definitive erythropoiesis in double KO mice compared to the single *Klf1* null littermates is accompanied by an increased number of functional CMEIs in the fetal liver, which indicates a prolonged survival of the erythroblastic

islands. The apoptotic program, perturbed in the fetal liver of *Klf1* null embryos, is more similar to the WT control. This improvement in definitive erythropoiesis, however, is not sufficient for the complete rescue of *Klf1* null embryos that are nevertheless strongly anemic and die by E16.5.

These data may contribute to better understand the role of *Klf1* in definitive erythropoiesis. Our results could also have implications on strategies for β -hemoglobinopathy therapies that target transcription factors involved in γ -globin repression [17, 18] such as *Klf1* [19]. In addition, the knowledge of the precise pathophysiology of *Klf1* shortage may improve the counseling and therapy of the pathologies caused by *Klf1* mutations, including fetal hydrops [20].

Table 1 Influence of the deficiency in interferon type I receptor on the survival of *Klf1*^{-/-}*Ifnar1*^{-/-} mice

Litter age ^a	<i>Klf1</i> ^{-/-} <i>Ifnar1</i> ^{+/+}		<i>Klf1</i> ^{-/-} <i>Ifnar1</i> ^{-/-}	
	Alive	Dead	Alive	Dead
E 14.5	5	0	6	0
E 15.5	0	4	3	0
E 16.5	0	0	0	5

^aThe morning of vaginal plug discovery was designated E0

Results

Partial rescue of *Klf1* KO mice

In this study, we aimed to determine if the type I interferon response contributes to the lethal anemia of the *Klf1* null phenotype by inactivating *IFN- β* in CMEIs. To this end we crossed *Klf1*^{+/-} mice with mice deficient in *Ifnar1*, which

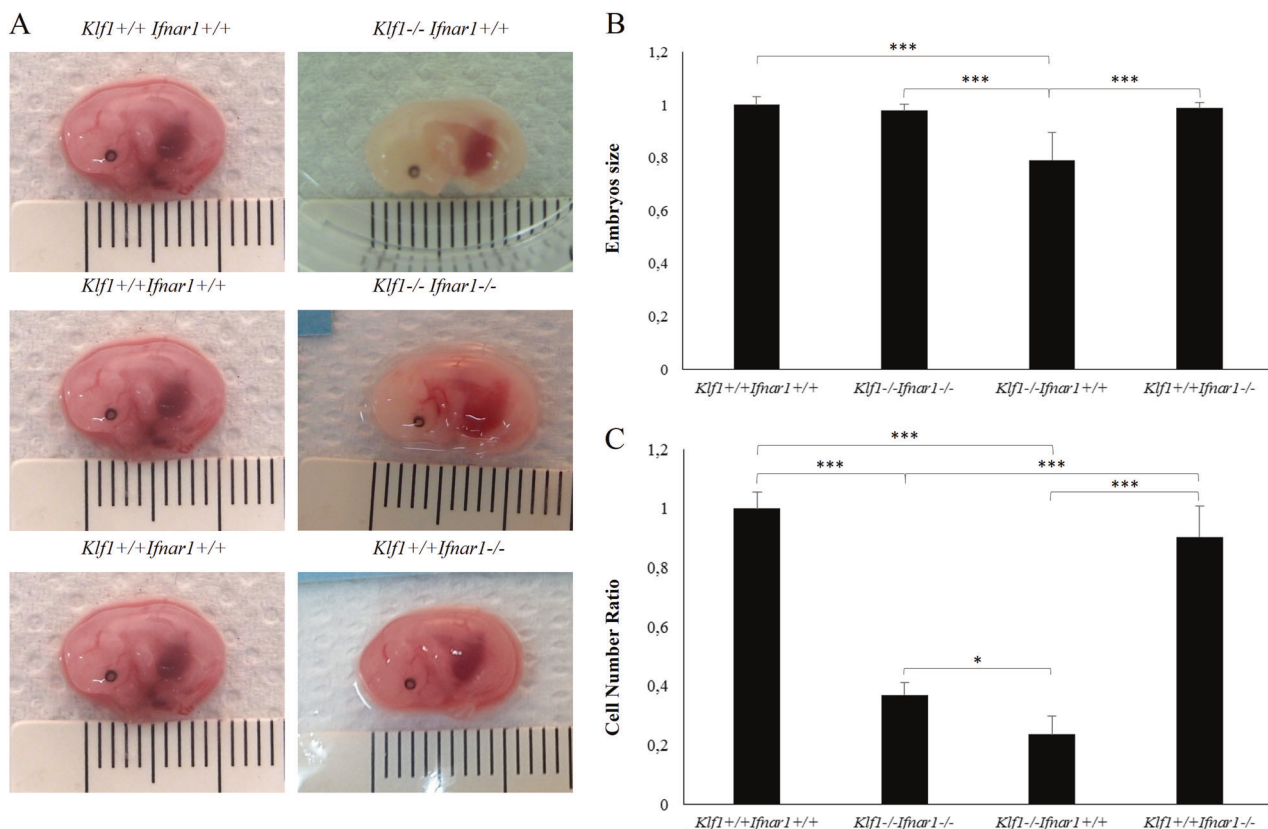


Fig. 1 Partial rescue of *Klf1* knockout mice by inactivation of *Ifnar1*. **a** Comparative E14.5 embryos morphology of different *Klf1* and *Ifnar1* genotypes as indicated. **b** E14.5 embryos size comparison among

different *Klf1* and *Ifnar1* genotypes as indicated in the histogram. **c** E14.5 fetal liver cell number. Ratio of each genotype with WT is reported. *Klf1* and *Ifnar1* genotypes as indicated in the histogram

encodes the common receptor for IFN- α and IFN- β . IFN- α is not activated in *Klf1*^{-/-} mice fetal liver [8].

Since *Ifnar1*^{-/-} mice develop normally [21], we generated and intercrossed *Klf1*^{+/-}*Ifnar1*^{-/-} mice. As a control, we intercrossed *Klf1*^{+/-}*Ifnar1*^{+/+} mice.

Genotype analysis of 130 newborn mice from *Klf1*^{+/-}*Ifnar1*^{-/-} intercrosses indicated that *Ifnar1* deficiency does not rescue the in utero lethality caused by *Klf1* absence.

To verify the possibility of a partial rescue with a prolonged in utero survival of the embryos we evaluated the embryos from E14.5 onwards (Table 1). At E14.5 the homozygous *Klf1*^{-/-}*Ifnar1*^{+/+} is severely anemic (Fig. 1a). Compared to the WT littermates, the embryo was smaller (75.42 \pm SD 8.2%, $p \leq 0.001$), extremely pale and no blood vessels are visible (Fig. 1a, b) [1, 2]. Otherwise, embryos with a double deficiency for *Klf1* and *Ifnar1* were equal in size to the *Klf1*^{+/+}*Ifnar1*^{-/-} littermates ($p = 0.64$), and although paler, some blood vessels were visible (Fig. 1a, b). *Klf1*^{-/-}*Ifnar1*^{+/+} were also significantly smaller than *Klf1*^{-/-}*Ifnar1*^{-/-} and *Klf1*^{+/+}*Ifnar1*^{-/-} embryos ($p \leq 0.001$) (Fig. 1b). On the other hand no statistically significant difference in size was detected among *Klf1*^{+/+}*Ifnar1*^{+/+}, *Klf1*^{-/-}*Ifnar1*^{-/-}, and *Klf1*^{+/+}*Ifnar1*^{-/-} embryos (Fig. 1b).

Klf1^{-/-}*Ifnar1*^{-/-} fetal livers appear bigger and less pale compared to *Klf1*^{-/-}*Ifnar1*^{+/+} fetal livers (Fig. 1a and data not shown).

To assess the potential improvement in fetal liver cellularity we normalized the number of E14.5 fetal liver cells of each genotype to that of *Klf1*^{+/+}*Ifnar1*^{+/+} embryos (Fig. 1c). The cellularity of *Klf1*^{-/-}*Ifnar1*^{-/-} was more than 35% (0.37 \pm SD 0.04) higher than that of *Klf1*^{-/-}*Ifnar1*^{+/+} (0.23 \pm SD 0.10) ($p = 0.0212$), however it was significantly lower than *Klf1*^{+/+}*Ifnar1*^{-/-} (0.90 \pm SD 0.10) and *Klf1*^{+/+}*Ifnar1*^{+/+} (1.00 \pm SD 0.056) embryos (Fig. 1c; $p \leq 0.001$). No statistically significant difference was detected between *Klf1*^{+/+}*Ifnar1*^{-/-} and *Klf1*^{+/+}*Ifnar1*^{+/+} embryos (Fig. 1c).

This result indicates an improvement of the fetal liver development in *Klf1*^{-/-}*Ifnar1*^{-/-} compared to *Klf1*^{-/-}*Ifnar1*^{+/+} embryos.

At E15.5 there was an improvement in the survival of *Klf1*^{-/-}*Ifnar1*^{-/-} embryos with respect to *Klf1*^{-/-}*Ifnar1*^{+/+}. *Klf1*^{-/-}*Ifnar1*^{-/-} embryos were paler than *Klf1*^{+/+}*Ifnar1*^{-/-} littermates but otherwise developmentally normal and alive. At this stage, the *Klf1*^{-/-}*Ifnar1*^{+/+} were all dead (no heartbeat) [1]. By day 16.5 *Klf1*^{-/-}*Ifnar1*^{-/-} embryos were dead (no heartbeat) (Table 1).

These data demonstrate a prolonged in utero survival of the *Klf1*^{-/-}*Ifnar1*^{-/-} embryos compared to the *Klf1*^{-/-}*Ifnar1*^{+/+} embryos, accompanied by an improvement of fetal liver development.

Definitive erythropoiesis and enucleation are improved in *Klf1*^{-/-} *Ifnar1*^{-/-} mice fetal liver

To investigate whether the ameliorated phenotype of *Klf1*^{-/-}*Ifnar1*^{-/-} compared to *Klf1*^{-/-}*Ifnar1*^{+/+} embryos was accompanied by an improvement in the fetal liver erythropoiesis, we analyzed, by flow cytometry, E14.5 fetal liver cells. *Ifnar1* expression is not affected by *Klf1* deprivation in the E14.5 fetal liver (see Supplementary Information).

Klf1^{-/-}*Ifnar1*^{+/+} and *Klf1*^{-/-}*Ifnar1*^{-/-} mice lack Ter119 expression (see Supplementary Information) [6, 22]. To date, CD44 transcription has not been reported to be influenced by *Klf1* deprivation in mouse fetal liver cells [22]. However, CD44 is reported to be affected by Klf1 in human erythrocytes [23–25]. To determine if the expression of CD44 gene is affected by the absence of *Klf1* in mouse, using flow cytometry, we compared, CD44 expression level in WT and *Klf1*^{-/-}*Ifnar1*^{+/+} fetal liver cells from E14.5 samples (Fig. 2a). *Klf1* KO fetal liver cells showed a clearly detectable expression of CD44. Therefore, CD45 and PI negative fetal liver cells were analyzed with CD44 and cell size as markers [23, 24] (Fig. 2b). Proerythroblasts (CD44^{hi}Ter119^{low}) were excluded from the analysis since the lack of Ter119 hampers their unambiguous identification [26,27].

We considered three different populations: Population II (PII), represented by basophil erythroblasts (big cell size, CD44 + + +), Population III (PIII), represented by polychromatic erythroblasts (medium cell size, CD44 + +) and Population IV (PIV), orthochromatic erythroblasts (small cell size, CD44 +) (Fig. 2b) [26, 27]. The same genotypes were analyzed by hematoxylin/eosin staining on E14.5 fetal liver slides (Fig. 2c).

First, we compared the pattern of differentiation among WT and *Klf1*^{+/+}*Ifnar1*^{-/-} cells. Flow cytometry highlights an identical expression profile (Fig. 2b) and no morphological differences in the histologic examination of hematoxylin/eosin fetal liver (Fig. 2c), demonstrating that no alteration had taken place due to the lack of *Ifnar1* response during erythropoiesis.

Analysis of *Klf1*^{-/-}*Ifnar1*^{+/+} mice fetal liver cells by flow cytometry showed higher heterogeneity compared to the WT in terms of cell size and CD44 level of expression (Fig. 2b). Hematoxylin/eosin staining showed a general impairment of the tissue (Fig. 2c) with the increase of interstitial space between cells (arrows) compared to other genotypes and likely alteration of the extracellular matrix. A predominance of hematopoietic cells can be seen in the liver from WT mice. The density of these cells is similar in the *Klf1*^{+/+}*Ifnar1*^{-/-} liver. In the *Klf1*^{-/-}*Ifnar1*^{+/+} liver, cell density is reduced and several cells showed degenerative changes like condensed nuclei.

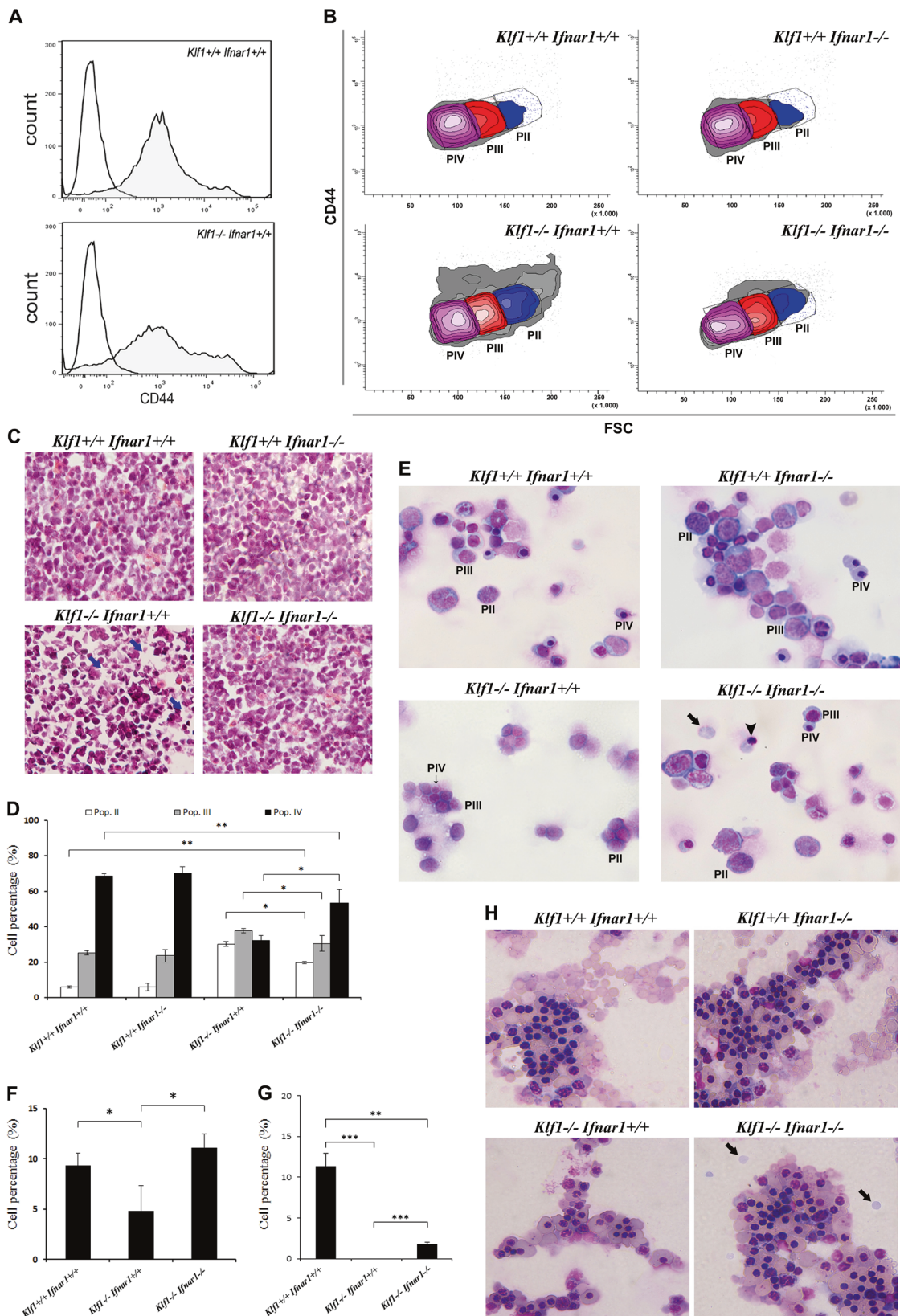


Fig. 2 Improvement of fetal liver definitive erythropoiesis. **a** Histograms representing flow cytometry of CD44 labeled freshly isolated fetal liver cells from E14.5 mice showing the comparison between *Klfl1*^{+/+}*Ifnar1*^{+/+} (upper histogram) and *Klfl1*^{-/-}*Ifnar1*^{+/+} (lower histogram) level of expression of CD44 marker. **b** FACS analysis of normoblastic population of E14.5 fetal liver cells on *Klfl1*^{+/+}*Ifnar1*^{+/+}, *Klfl1*^{+/+}*Ifnar1*^{-/-}, *Klfl1*^{-/-}*Ifnar1*^{+/+}, and *Klfl1*^{-/-}*Ifnar1*^{-/-} genotypes. Populations II, III, and IV are labeled as PII, PIII, and PIV and are evidenced by blue, orange, and purple color respectively. **c** Hematoxylin/eosin staining of E14.5 fetal liver slides from same genotypes as in **b**. Arrows indicate interstitial space. Magnification: 20X. **d** Percentages of P II, III, IV, of same genotypes as in **b** from CD44 Vs FSC flow cytometry analysis (*p*-value: * ≤ 0.05; ** ≤ 0.01). **e** Cytospin images of fetal liver cells suspensions from same genotypes as in **b**. Black head arrow indicating an enucleating orthochromatic normoblast, black arrow indicating a reticulocyte. Magnification: 60X. **f** Bar chart representing percentage of fetal liver enucleating orthochromatic erythroblast from cytospin of *Klfl1*^{+/+}*Ifnar1*^{+/+} (22 fields, a total of 637 cells) *Klfl1*^{-/-}*Ifnar1*^{+/+} (51 fields, a total of 1385 cells), and *Klfl1*^{-/-}*Ifnar1*^{-/-} (41 fields a total of 1080 cells), genotypes (*p*-value: * ≤ 0.05). **g** Quantification of percentage of reticulocytes from cytospin of *Klfl1*^{+/+}*Ifnar1*^{+/+} (39 fields, a total of 807 cells), *Klfl1*^{-/-}*Ifnar1*^{+/+} (44 fields, a total of 929 cells), and *Klfl1*^{-/-}*Ifnar1*^{-/-} (62 fields, a total of 1310 cells) fetal liver cells (*p*-value: ** ≤ 0.01; *** ≤ 0.001). **h** Cytospin of peripheral blood from same genotypes as in **b** (black arrow indicate enucleated cells). Magnification: 40X

In *Klfl1* KO samples lacking *Ifnar1* expression, flow cytometry analysis highlighted less cellular heterogeneity and had a plot more similar to the WT (Fig. 2b). Hematoxylin/eosin staining demonstrated a substantial improvement of the fetal liver architecture. *Klfl1*^{-/-} *Ifnar1*^{-/-} liver histology resembled that of WT mice with restoration of extracellular matrix. The density of the hematopoietic cells was similar to that of *Klfl1*^{+/+}*Ifnar1*^{-/-} and WT liver (Fig. 2c).

Quantitation of the three erythroblast populations among WT and *Klfl1*^{+/+}*Ifnar1*^{-/-} showed no differences in the pattern of differentiation (Fig. 2d). Quantitative comparison between *Klfl1*^{-/-} *Ifnar1*^{-/-}, *Klfl1*^{-/-}*Ifnar1*^{+/+}, and WT fetal liver cell populations showed a significant difference in the three erythroblast populations and highlighted a partial recovery of the normal kinetic of the erythropoiesis in the *Klfl1*^{-/-}*Ifnar1*^{-/-} fetal liver compared to *Klfl1*^{-/-}*Ifnar1*^{+/+} mice (Fig. 2d). Populations II, III and IV remained virtually flat in *Klfl1*^{-/-}*Ifnar1*^{+/+} fetal liver (PII: 30.3% ± SD 1.4; PIII: 37.9% ± SD 1.3 and PIV: 32.2% ± SD 2.8) while in *Klfl1*^{-/-}*Ifnar1*^{-/-} fetal liver they showed a progressive increase (PII: 19.7% ± SD 0.57; PIII: 30.6% ± SD 4.4 and PIV: 53.4% ± SD 7.5). These percentages are significantly different from the *Klfl1* null mice as well as from the WT control (PII: 6.1% ± SD 0.48; PIII: 25.3% ± SD 1.2 and PIV: 68.6% ± SD 1.4) (Fig. 2d) but showed a partial restoration of the normal erythropoiesis where erythroblast differentiation is coupled to proliferation, which is missing in the *Klfl1*^{-/-}*Ifnar1*^{+/+} fetal liver.

Cytospin analysis of *Klfl1*^{-/-}*Ifnar1*^{-/-} fetal liver cells revealed the presence of the entire repertoire of erythroblasts population (Fig. 2e) including late stage enucleating orthochromatic erythroblasts (Fig. 2e, black head arrow) and enucleated reticulocytes (Fig. 2e, black arrow). Cytospin of *Klfl1*^{-/-}*Ifnar1*^{+/+} fetal liver cells evidenced the presence of the three erythroblastic populations but no reticulocytes were detected (Fig. 2e), confirming recent reports [7]. We quantified the proportion of enucleating orthochromatic erythroblasts and reticulocytes from cytospin in fetal liver of the different genotypes. We identified as “enucleating orthochromatic erythroblasts” cells with an elongated shape and with an asymmetric or protruding nuclei. As shown in Fig. 2f, the percentage of enucleating orthochromatic in *Klfl1*^{-/-}*Ifnar1*^{+/+} fetal liver was significantly decreased compared to WT (4.8% ± SD 2.4 vs. 9.3% ± SD 1.7; *p* = 0.026). On the other hand the proportion of enucleating orthochromatic was re-established in *Klfl1*^{-/-}*Ifnar1*^{-/-} fetal liver (11.1% ± SD 1.4; *p* = 0.14) and was significantly different from the *Klfl1*^{-/-}*Ifnar1*^{+/+} fetal liver (*p* = 0.023). Furthermore, reticulocytes could also be detected in the fetal liver (Fig. 2e), although at a reduced number compared to the WT (1.8% ± SD 0.2 vs. 11.4% ± SD 1.6; *p* = 0.0023) (Fig. 2g), while they are undetectable in *Klfl1*^{-/-}*Ifnar1*^{+/+} fetal liver (Fig. 2g).

Cytospin of peripheral blood confirmed the presence of enucleated cells in *Klfl1*^{-/-}*Ifnar1*^{-/-} mice (Fig. 2h), which are absent in *Klfl1*^{-/-}*Ifnar1*^{+/+} peripheral blood (Fig. 2h).

A number of erythroid genes targeted by *Klfl1* were also analyzed by RT-qPCR (see Supplementary Information). None of the analyzed genes was increased to a level that may have contributed to the observed improvement in definitive erythropoiesis.

In summary, flow cytometry, hematoxylin/eosin staining, and cytospin analysis demonstrated an improvement of *Klfl1* KO erythropoiesis, with partial restoration of enucleation in mice lacking *Ifnar1* expression.

Improvement in fetal liver CMEI

In *Klfl1* null mice, CMEI are strongly compromised in number and shape and *IFN-β* is activated [8]. We wished to evaluate if the observed improvement of definitive erythropoiesis in *Klfl1*^{-/-}*Ifnar1*^{-/-} could be associated with an improvement of CMEI. Immunofluorescence analysis using F4/80 showed the distribution and morphological features of macrophage cells in mouse fetal liver (Fig. 3a). Interestingly, when we quantified the distribution of macrophage populations, we observed a significant increase of the average number per field of F4/80 positive macrophages in *Klfl1*^{-/-}*Ifnar1*^{-/-} compared to *Klfl1*^{-/-}*Ifnar1*^{+/+}, (18.2 ± SD 2.21 vs. 13.6 ± SD 0.28, respectively, *p* = 0.022), (Fig. 3b). Quantitative assessment of F4/80 positive cells by

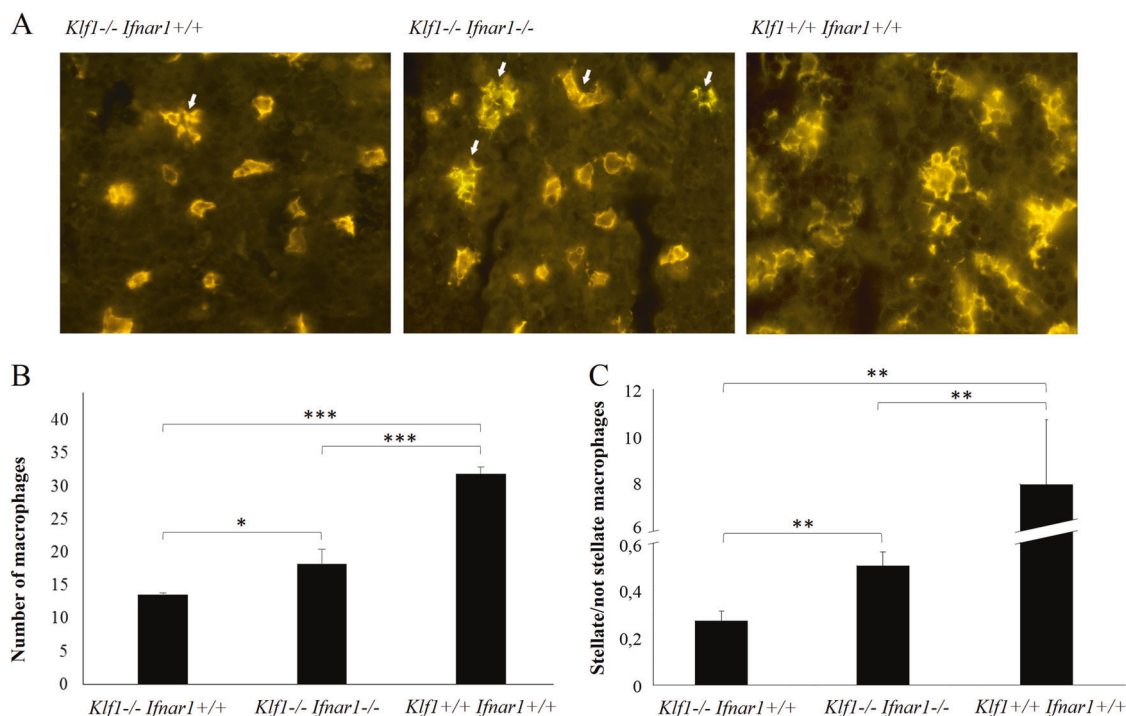


Fig. 3 Improvement in fetal liver CMEIs. **a** Histological assay on E14.5 *Klf1*^{-/-} *Ifnar1*^{+/+}, *Klf1*^{-/-} *Ifnar1*^{-/-} and *Klf1*^{+/+} *Ifnar1*^{+/+} fetal liver sections. Arrows indicate macrophages with normal morphology. Scale bar = 30 μm. **b** The diagram shows the number of macrophages/field in E14.5 *Klf1*^{-/-} *Ifnar1*^{+/+}, *Klf1*^{-/-} *Ifnar1*^{-/-} and

Klf1^{+/+} *Ifnar1*^{+/+} fetal liver sections. **c** The diagram shows the ratio between stellate and non stellate macrophages morphology in E14.5 *Klf1*^{-/-} *Ifnar1*^{+/+}, *Klf1*^{-/-} *Ifnar1*^{-/-}, and *Klf1*^{+/+} *Ifnar1*^{+/+} fetal liver sections

FACS confirmed the increased number of macrophages in *Klf1*^{-/-} *Ifnar1*^{-/-} compared to *Klf1*^{-/-} *Ifnar1*^{+/+} (see Supplementary Information).

In our previous study [8], we observed two morphologically different types of fetal liver macrophages. In mice with the *Klf1*^{+/+} genotype, we identified cells showing typical morphology, with extensive cytoplasmic projections (stellate macrophages) [28, 29] while smaller and rounder macrophages without cytoplasmic protrusions (non stellate macrophages), were mainly observed in *Klf1*^{-/-} fetal livers.

In this work, we identified an increased proportion of macrophages showing normal morphology, with extensive cytoplasmic projection, in *Klf1*^{-/-} *Ifnar1*^{-/-} compared to *Klf1*^{-/-} *Ifnar1*^{+/+} (Fig. 3a). The ratio between macrophages with a classical stellate morphology in comparison to non-stellate morphology was almost double in *Klf1*^{-/-} *Ifnar1*^{-/-} compared to *Klf1*^{-/-} *Ifnar1*^{+/+} E14.5 fetal liver (0.50 ± SD 0.06 vs. 0.26 ± SD 0.04, respectively, $p = 4.6 \times 10^{-3}$), (Fig. 3c).

These results suggest that the improved definitive erythropoiesis in *Klf1*^{-/-} *Ifnar1*^{-/-} compared to *Klf1*^{-/-} *Ifnar1*^{+/+} embryos is associated with prolonged survival of the CMEI and of the associated erythroblastic islands.

Improvement of the apoptotic program

Apoptotic mechanisms play a relevant role in the control of erythropoiesis [30, 31]. Recent evidence has shown that the apoptotic gene expression pattern is perturbed in the absence of *Klf1* [32]. It has been suggested that the distorted apoptotic genetic program may contribute to the failure of terminal erythroid differentiation in *Klf1* null mice [32]. In particular, Caspase-3 has been shown to be activated in *Klf1* null erythroid cells [32]. We have carried out western blotting analysis of whole-cell E14.5 fetal liver protein extract of WT, *Klf1*^{+/+} *Ifnar1*^{-/-}, *Klf1*^{-/-} *Ifnar1*^{+/+}, and *Klf1*^{-/-} *Ifnar1*^{-/-} embryos using a specific antibody for activated murine Caspase-3 and Actin as loading control. As shown in Fig. 4a, only in *Klf1*^{-/-} *Ifnar1*^{+/+} fetal liver cells is there evidence of the 17 and 19 KD forms of activated Caspase-3, which are absent in the other genotypes, including *Klf1*^{-/-} *Ifnar1*^{-/-}.

We looked for additional hallmarks of improvement of the apoptotic program. We carried out a TUNEL assay on E14.5 CD71 + fetal liver erythroid population. As shown in Fig. 4b and c, a significant increase of the percentage of apoptotic cells (6.3% ± SD 0.55) is observed in *Klf1*^{-/-} *Ifnar1*^{+/+} embryos compared to the other genotypes ($p \leq 0.001$). It is notable that the percentage of TUNEL positive

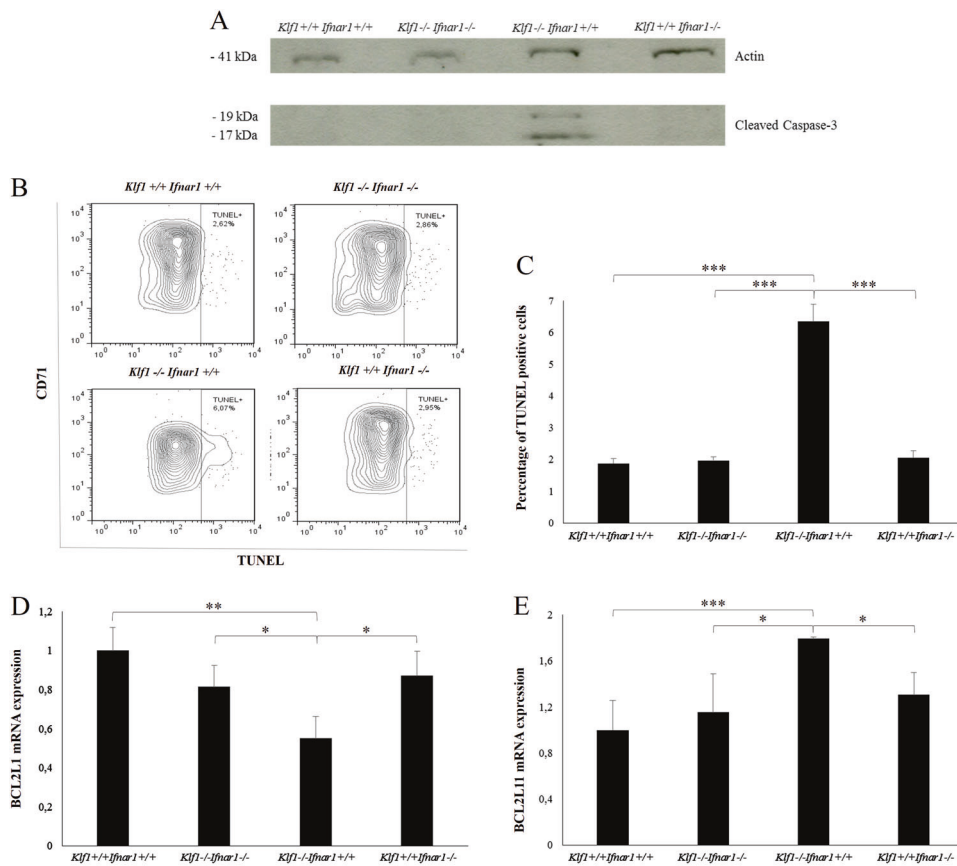


Fig. 4 Improvement of the apoptotic program. **a** Western blotting analysis of whole-cell protein extracts of different *Klf1* and *Ifnar1* genotypes as indicated. Protein levels of Cleaved Caspase-3 were investigated using specific antibody with Actin as a loading control. Cleavage products of Caspase-3 occur only in *Klf1*^{-/-}*Ifnar1*^{+/-} mice. **b** Representative TUNEL assay FACS plots for the four genotypes as

indicated. Cells were co-stained for TUNEL and CD71 **c**. Bar chart representing the percentage of cells staining TUNEL positive in the four genotypes as indicated. **d** Expression level of the anti-apoptotic *Bcl2l1* gene; genotypes are indicated in the histogram. **e** Expression level of the pro-apoptotic *Bcl2l11* gene; genotypes are indicated in the histogram

cells is decreased in *Klf1*^{-/-}*Ifnar1*^{-/-} embryos (1.96 ± SD 0.13) to a level not significantly different from WT and *Klf1*^{+/-}*Ifnar1*^{-/-} control embryos (1.88% ± SD 0.14 and 2.06% ± SD 0.21; respectively).

Moreover, we have analyzed by RT-qPCR, the expression level of the anti-apoptotic *Bcl2l1* gene, suggested to be a target of *Klf1* [33] and downregulated in *Klf1* null fetal liver embryos [32], and of the pro-apoptotic *Bcl2l11* gene, a critical determinant of erythroid cell survival that is upregulated in *Klf1* null fetal liver embryos [32]. As shown in Fig. 4d, e, a significant down regulation of *Bcl2l1* (0.55 ± SD 0.11) and up regulation of *Bcl2l11* (1.79 ± SD 0.016) in *Klf1*^{-/-}*Ifnar1*^{+/-} embryos compared to the WT ($p \leq 0.001$) are observed, in agreement with previous results [32]. On the other hand no significant difference in the expression level of these two genes was been detected among *Klf1*^{-/-}*Ifnar1*^{-/-}, *Klf1*^{+/-}*Ifnar1*^{-/-} and WT embryos (Fig. 4d, e).

These results indicate a significant re-establishment of the normal apoptotic program in *Klf1* null mice lacking the

Interferon type I receptor. These data support the notion that Interferon-β response, through *Ifnar1*, contributes to the perturbation of the apoptotic program seen in *Klf1* null mice.

Discussion

The most obvious effect of *Klf1* deprivation in mice is lethal β-thalassemia [1, 2]. However, rescue of globin imbalance does not rescue the lethal phenotype, suggesting a major role of *Klf1* in definitive erythropoiesis [34].

In our previous work, we have shown that *Dnase2* is strongly downregulated in the fetal liver of *Klf1* KO mice and that *IFN-β* is activated in CMEI [8]. The inhibitory effect of *IFN-β* on erythropoiesis has been known for decades [35]. Here, we reasoned that the absence of the *Ifnar1* gene, by hampering the activation of Interferon-β response in the fetal liver, could lead to an amelioration of the *Klf1* null phenotype in mice. To verify our hypothesis we

crossed *Klf1*^{+/-} mice with mice deficient in *Ifnar1*, which encodes the common receptor for IFN- α and IFN- β , to obtain *Klf1*^{-/-}*Ifnar1*^{-/-} double-deficient mice.

Earlier reports have shown that in *Klf1* null mice terminal erythroid differentiation is absent [6]. More recently, some works have indicated that in *Klf1*^{-/-} mice the definitive erythropoiesis proceeds beyond the initial block at the progenitor stage allowing attainment of the orthochromatic erythroblast stage, but with a failure to enucleate [7]. Here, we show that in the absence of the type I Interferon receptor the erythroid differentiation is consistently improved in *Klf1* null mice. Terminal erythroid differentiation is a process through which proliferation is linked to differentiation. For every mitosis, distinct populations of erythroblasts are produced. Proerythroblasts undergo three mitoses to sequentially generate basophilic, polychromatic, and orthochromatic erythroblasts. In normal murine terminal erythroid differentiation, a kinetic of a progressive increase of the populations is expected. In *Klf1* null mice this progression is completely abolished in the E14.5 fetal liver. On the other hand, in *Klf1*^{-/-}*Ifnar1*^{-/-} double-deficient mice, the normal kinetic of fetal liver erythropoiesis is partially re-established with a significant progressive increase of the erythroblastic populations closer to the physiological pattern (Fig. 5).

This result suggests that in absence of *Klf1*, the impairment of definitive erythropoiesis is not only due to a direct effect of Klf1 on erythropoiesis, but also to a secondary effect due to Interferon- β activation in CMEI. The slower differentiation rate is most likely caused by a partial failure of erythroid specific cell cycle control due to the absence of *Klf1* [6, 7, 36]. β -globin imbalance (β -thalassemia) may also

contribute to the decreased differentiation of erythroid cells [37].

Notably, in absence of the Interferon type I receptor, *Klf1*^{-/-} orthochromatic erythroblasts are able to enucleate and produce reticulocytes, even though to a lesser extent than the WT control. This result indicates that *Klf1*^{-/-} erythroblasts are able to partially overcome the stall at the orthochromatic stage [7] and to produce some reticulocytes that enter the blood stream. This block at the orthochromatic stage is proposed to be caused by the downregulation of Klf1 cell cycle target genes, p18 and p27 [7]. We have shown that the partial recovery of enucleation in *Klf1*^{-/-}*Ifnar1*^{-/-} double-deficient mice is not linked to the recovery of either p18 or p27 expression (see Supplementary Information). Most likely this result is related to the amelioration of CMEI, and of the associated blood island, which is pivotal for efficient enucleation [10–12]. The improvement in definitive erythropoiesis and enucleation is indeed associated with a partial recovery of the absolute number and shape of macrophages in the *Klf1*^{-/-}*Ifnar1*^{-/-} fetal liver compared to *Klf1*^{-/-}*Ifnar1*^{+/+} mice. These data indicate a prolonged survival of the CMEIs and of the associated erythroblastic islands. However, the ratio between stellate and non-stellate macrophages, although higher than that of the single *Klf1* KO, is inferior of the WT control mice. These results are in agreement with the notion that Klf1 plays an important direct role in erythroblastic island biology and integrity [38–40].

Our data also suggest that the previously observed perturbation of the apoptotic program [32], is caused, at least in part, by IFN- β activation in *Klf1* null fetal liver. The perturbation of the apoptotic program has been suggested to contribute to the failure of terminal erythroid differentiation in *Klf1* null mice [32]. Our data support the idea that the lack of *Ifnar1*, by hampering IFN- β -induced apoptosis, is the main cause of the observed improvement of erythroid differentiation in *Klf1*^{-/-}*Ifnar1*^{-/-} mice. Moreover, we have shown that the observed improvement in definitive erythropoiesis of *Klf1*^{-/-}*Ifnar1*^{-/-} compared to *Klf1*^{-/-}*Ifnar1*^{+/+} is not directly due to an increase in the expression of key Klf1 target genes (see Supplementary Information).

Unlike the nucleated erythroid cells produced in the yolk sac, those produced in the fetal liver and bone marrow are enucleated. Definitive erythropoiesis in both bone marrow and fetal liver takes place in erythroblastic islands [10, 11]. In *Klf1* null mice the primitive embryonic erythropoiesis allows the embryos to survive until the fetal liver definitive erythropoiesis takes place, even though most of the genes affected by *Klf1* deprivation are expressed in embryonic as well as definitive erythroid cells [22]. The absence of CMEI, with the consequential lack of IFN- β production in *Klf1* null primitive erythropoiesis, may partially explain this difference. Globin imbalance also certainly contributes to

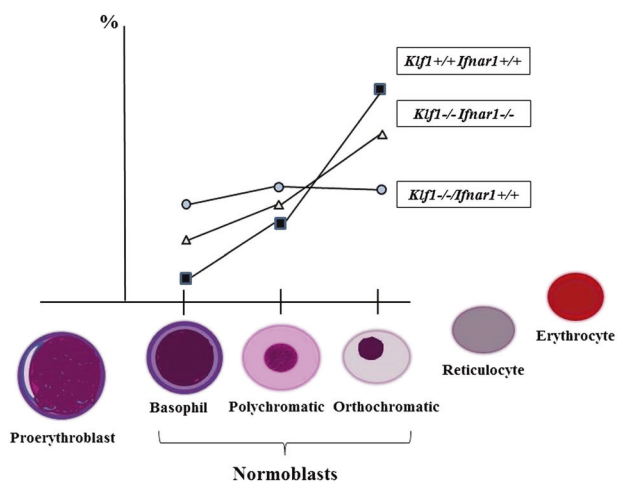


Fig. 5 Schematic representation of erythropoiesis analyzed by flow cytometry in *Klf1*^{+/+}*Ifnar1*^{+/+}, *Klf1*^{-/-}*Ifnar1*^{+/+}, and *Klf1*^{-/-}*Ifnar1*^{-/-} E14.5 mice fetal liver cells through CD44 level expression and forward scatter as marker

the difference in the level of impairment of erythropoiesis between primitive and definitive erythroid production.

The central role of Klf1 in erythropoiesis is confirmed by our study, which however highlights a contribution of IFN- β that exacerbates the *Klf1* null phenotype in mice. The overlap of direct and secondary effects could have given rise to an over-estimation of some aspect of Klf1's role in erythrocyte development. In this study we have shown that in the absence of *Ifnar1*, which mediates the cellular response to IFN- β , erythropoiesis and enucleation are significantly improved in the E14.5 *Klf1* null fetal liver.

Recent studies have shown that mutations of *Klf1* are not rare, are under selection, and in some populations may reach appreciable frequencies [20]. *Klf1* mutations result in a spectrum of serious diseases up to hydrops fetalis [3], which, although rare, is probably underestimated. In this respect, the knowledge of the pathophysiological mechanisms underlying *Klf1* null phenotype may help for an effective counseling and therapeutic approach of these diseases.

In this report, we have shown that the absence of IFN- β cellular response attenuate the *Klf1* null phenotype. We hypothesize that a further amelioration of erythropoiesis in *Klf1*-/*Ifnar1*- mice would be realized if the globin imbalance were corrected, but this remains to be established. However, if this is indeed the case, Klf1 could be re-evaluated as a target for γ -globin gene reactivation as a therapy for β -thalassemia and sickle cell disease [17–19].

Material and methods

Mice

The original *Klf1* KO (provided by Dr. Frank Grosveld's laboratory [1]) and *Ifnar1* KO (bought from Riken Bio Resource Center, Japan) mouse lines were maintained on a hybrid C57BL/6/CBA/J background. Evaluation of the embryos size has been carried out on at least three pregnancies and four embryos per genotype. Evaluation of fetal liver cellularity has been carried out on at least two pregnancies and three embryos per genotype. Evaluation of the in utero survival has been carried out on at least two pregnancies and three embryos per genotype.

All procedures conducted on the animals were in accordance to the rules and regulations set by the Ethical Committee (OPBA) of University of Cagliari (Approval number: 13/2016).

Genotyping

Genotypes were determined by PCR from genomic DNA using a pair of primers in the *neomycin-resistant* gene (*NeoI*

Fw 5'-ATGGGATCGGCCATTGAAC-3'; *Neo/Rev* 5'-CTCGTCCTGCAGTTCATTC-3') and a pair of primers in the *Klf1* gene (*Klf1/Fw* 5'-CCACACACATATCGCACAC-3'; *Klf1/Rev* 5'-TGCCGCCTCCACACACACTC-3') to discriminate between the WT and KO *Klf1* gene.

WT and *Ifnar1* KO were detected with a wild-type-specific (5'-AAGATGTGCTGTTCCCTTCCTCTGCTCTGA-3') or mutant-specific (5'-CCTGCGTGCAATCCATCTTG-3') reverse primer and a common forward primer (5'-ATTATTAAGAAAAGACGAGGCGAAGTGG-3').

Real-time quantitative PCR (RT-qPCR)

Total RNA was extracted from E14.5 fetal livers using RNeasy Mini Kit (Qiagen) as described by the manufacturer's protocol. The cDNA was made from total RNA using Superscript III reverse transcriptase (Invitrogen). RT-qPCRs were performed using SYBR Green chemistry (Applied Biosystems) by ABI PRISM 7900 thermocycler (Applied Biosystems, Foster City, CA).

The reactions were performed at least on three different samples in triplicate. See additional data for primers sequence. Samples were normalized with respect to *HPRT* levels. The analysis of RT-qPCR data was done using the $\Delta\Delta CT$ method.

Flow cytometry analysis

Freshly isolated E14.5 fetal liver cells (at least three samples per genotype) were collected and stained with anti-mouse CD44 FITC, and anti-mouse CD45 PE antibodies (BD-Bioscience) at a final concentration 1:100. Cells were incubated for 20 min at 4 °C. Stained cells were then washed with PBS (5% BSA) and resuspended in FACS buffer. Propidium Iodide (BD Pharmingen) were added and incubated for 10 min at room temperature. Data were collected on a FACSCANTO flow cytometer (BD-Bioscience) and analyzed with FACSDiva software Version 6.1.3 (BD Biosciences) and FloJo V7.6.5.

Histochemical analysis

The fetal liver samples obtained from E14.5 mice (at least three samples per genotype) were fixed with 4% paraformaldehyde, included in an embedding medium [41] and cut (at 10 μ m) using a HM-560 cryomicrotome (Micom; Walldorf, Germany). Sections were incubated overnight with rat anti-mouse F4/80 (MCA497R; AbD Serotec, Oxford, UK) monoclonal antibody (1:200) revealed with a secondary antibody conjugated with cyanine 3.18 (1:300, 60 min, Jackson ImmunoResearch Laboratories, West Grove, PA). Slides were observed and photographed using BX51 fluorescence microscope (Olympus, Milan, Italy)

equipped with the Fuji S3 Pro digital camera (Fujifilm, Milan, Italy). Routine controls included substitution of primary antibody with PBS and/or dilution buffer only. Quantitation of macrophages was then carried out on five non-adjacent sections per samples and 4/5 fields per section.

Morphological examination was made in fetal liver sections (at least three samples for genotype) stained with hematoxylin/eosin.

Cytospins were prepared with 5 μ l of fetal liver cells suspension (five mice per genotype, three slides per mouse) at a final concentration of 1×10^5 cell/ μ l. Slides were stained with Differential Quik Stain Kit (Modified Giemsa) (Polysciences, Inc.).

Western blotting

Fetal liver E14.5 whole-cell protein extracts were prepared using RIPA buffer and resolved on 4%-12% Bis-Tris precast gels (Invitrogen). Blotting was performed by transferring proteins to PVDF membrane (GE Healthcare), blocking, and incubating with the appropriate primary and a conjugated secondary antibody. The primary antibodies used were as follows: anti-Cleaved Caspase-3 (9661 Cell Signaling Technology) and anti-Actin, (sc-1616 Santa Cruz).

TUNEL (terminal deoxynucleotidyl transferase dUTP nick and labeling) assay

A cell suspension of E14.5 fetal liver cells were assayed for apoptosis using the TUNEL method (three samples per genotype). Cells were marked with anti-mouse CD71 PE (BD-Bioscience) antibody. Cells were prepared according to the manufacturer's recommendations using the In Situ Cell Death Detection Kit, Fluorescein (Roche). Analysis was carried out using a FACSCANTO flow cytometer (BD-Bioscience) and analyzed with FACSDiva software Version 6.1.3 (BD Biosciences) and FloJo V7.6.5.

Statistical analysis

Statistical differences between means were calculated with Student's *t*-test (Microsoft Excel).

Acknowledgements We thank Maria Franca Marongiu, Valeria Faa, and Paolo Moi for kindly reading the manuscript; Daniela Poddie, Alessia Desogus, and Alessia Loi for technical support, Emilio Melis for animal care and technical assistance and Michael Whalen for proofreading the manuscript. Professor Andrea Perra for histopathological examination of the fetal liver.

Authors' contributions M.F.M., C.B., C.A.C., E.M., M.S., I.A., S.P., and L.P. performed the experiments and contribute to the interpretation of the results. M.F.M., C.B., C.A.C., E.M., M.S., and S.P. contributed to the writing of the manuscript and prepared the figures. M.S.R. and M.F.M. designed the study. M.S.R. designed the study, supervised the

research and wrote the manuscript. All authors contributed to the discussion and approved the final manuscript.

Compliance with ethical standards

Competing interests The authors declare that they have no competing financial interests.

Open Access This article is licensed under a Creative Commons Attribution-NonCommercial-ShareAlike 4.0 International License, which permits any non-commercial use, sharing, adaptation, distribution and reproduction in any medium or format, as long as you give appropriate credit to the original author(s) and the source, provide a link to the Creative Commons license, and indicate if changes were made. If you remix, transform, or build upon this article or a part thereof, you must distribute your contributions under the same license as the original. The images or other third party material in this article are included in the article's Creative Commons license, unless indicated otherwise in a credit line to the material. If material is not included in the article's Creative Commons license and your intended use is not permitted by statutory regulation or exceeds the permitted use, you will need to obtain permission directly from the copyright holder. To view a copy of this license, visit <http://creativecommons.org/licenses/by-nc-sa/4.0/>.

References

1. Nuez B, Michalovich D, Bygrave A, Ploemacher R, Grosfeld F. Defective haematopoiesis in fetal liver resulting from inactivation of the EKLf gene. *Nature* 1995;375:316–8.
2. Perkins AC, Sharpe AH, Orkin SH. Lethal beta-thalassaemia in mice lacking the erythroid CACCC-transcription factor EKLf. *Nature* 1995;375:318–22.
3. Magor GW, et al. KLF1-null neonates display hydrops fetalis and a deranged erythroid transcriptome. *Blood* 2015;125(15):2405–17.
4. Tallack MR, Perkins AC. KLF1 directly coordinates almost all aspects of terminal erythroid differentiation. *IUBMB Life* 2010;62(12):886–90.
5. Siatecka M, Bieker JJ. The multifunctional role of EKLf/KLF1 during erythropoiesis. *Blood* 2011;118:2044–54.
6. Pilon AM, et al. Failure of terminal erythroid differentiation in EKLf deficient mice is associated with cell cycle perturbation and reduced expression of E2F2. *Mol Cell Biol* 2008;28(24):7394–401.
7. Gnanapragasam MN, McGrath KE, Catherman S, Xue L, Palis J, Bieker JJ. EKLf/KLF1-regulated cell cycle exit is essential for erythroblast enucleation. *Blood* 2016;128(12):1631–41.
8. Porcu S, et al. Klf1 affects DNase II- α expression in the central macrophage of a fetal liver erythroblastic island: a non-cell-autonomous role in definitive erythropoiesis. *Mol Cell Biol* 2011;31:4144–54.
9. Bessis M. Erythroblastic island, functional unity of bone marrow. *Rev Hematol* 1958;13:8–11.
10. Chasis JA, Mohandas N. Erythroblastic islands: niches for erythropoiesis. *Blood*. 2008;112:470–8.
11. Manwani D, Bieker JJ. The erythroblastic island. *Curr Top Dev Biol* 2008;82:23–53.
12. de Back DZ, Kostova EB, van Kraaij M, van den Berg TK, van Bruggen R. Of macrophages and red blood cells; a complex love story. *Front Physiol* 2014;30(5):9.
13. Kawane K, et al. Requirement of DNase II for definitive erythropoiesis in the mouse fetal liver. *Science* 2001;292:1546–9.
14. Yoshida H, Okabe Y, Kawane K, Fukuyama H, Nagata S. Lethal anemia caused by interferon- β produced in mouse embryos carrying undigested DNA. *Nat Immunol* 2005;6:49–56.

15. Evans CJ, Aguilera RJ. DNase II: genes, enzymes and function. *Gene* 2003;322:1–15.
16. Kitahara Y, Kawane K, Nagata S. Interferon-induced TRAIL-independent cell death in DNase II^{-/-} embryos. *Eur J Immunol* 2010;40(9):2590–8.
17. Sankaran VG. Targeting therapeutic strategies for fetal hemoglobin induction. *Hematology Am Soc Hematol Educ Program*. 2011;2011:459–65.
18. Bauer DE, Kamran SC, Orkin SH. Reawakening fetal hemoglobin: prospects for new therapies for the β -globin disorders. *Blood* 2012;120(15):2945–53.
19. Zhou D1, Liu K, Sun CW, Pawlik KM, Townes TM. KLF1 regulates BCL11A expression and gamma- to beta-globin gene switching. *Nat Genet* 2010;42(9):742–4.
20. Perkins A, et al. KLF1 Consensus Workgroup. Krüppeling erythropoiesis: an unexpected broad spectrum of human red blood cell disorders due to KLF1 variants. *Blood* 2016;127(15):1856–62.
21. Müller U, et al. Functional role of type I and type II interferons in antiviral defense. *Science* 1994;264(5167):1918–21.
22. Hodge D, et al. A global role for EKLF in definitive and primitive erythropoiesis. *Blood* 2006;107(8):3359–70.
23. Singleton BK, Burton NM, Green C, Brady RL, Anstee DJ. Mutations in EKLF/KLF1 form the molecular basis of the rare blood group In(Lu) phenotype. *Blood* 2008;112(5):2081–8.
24. Arnaud L, et al. A dominant mutation in the gene encoding the erythroid transcription factor KLF1 causes a congenital dyserythropoietic anemia. *Am J Hum Genet* 2010;87(5):721–7.
25. Helias V, et al. Molecular analysis of the rare in(Lu) blood type: toward decoding the phenotypic outcome of haploinsufficiency for the transcription factor KLF1. *Hum Mutat* 2013;34(1):221–8.
26. Chen K, Liu J, Heck S, Chasis JA, An X, Mohandas N. Resolving the distinct stages in erythroid differentiation based on dynamic changes in membrane protein expression during erythropoiesis. *Proc Natl Acad Sci U S A* 2009;106(41):17413–8.
27. Liu J, et al. Quantitative analysis of murine terminal erythroid differentiation in vivo: novel method to study normal and disordered erythropoiesis. *Blood*. 2013;121:e43–49.
28. Gordon S, Crocker PR, Morris L, Lee SH, Perry VH, Hume DA. Localization and function of tissue macrophages. *Ciba Found Symp* 1986;118:54–67.
29. Morris L, Graham CF, Gordon S. Macrophages in haemopoietic and other tissues of the developing mouse detected by the monoclonal antibody F4/80. *Development* 1991;112:517–26.
30. Testa U. Apoptotic mechanisms in the control of erythropoiesis. *Leukemia* 2004;18:1176–99.
31. Sarvothaman S, Undi RB, Pasupuleti SR, Gutti U, Gutti RK. Apoptosis: role in myeloid cell development. *Blood Res* 2015;50:73–79.
32. Tallack MR, et al. Novel roles for KLF1 in erythropoiesis revealed by mRNA-seq. *Genome Res* 2012;22(12):2385–98.
33. Tallack MR, et al. A global role for KLF1 in erythropoiesis revealed by CHIP-seq in primary erythroid cells. *Genome Res* 2010;20(8):1052–63.
34. Perkins AC, Peterson KR, Stamatoyannopoulos G, Witkowska HE, Orkin SH. Fetal expression of a human A gamma globin transgene rescues globin chain imbalance but not hemolysis in EKLF null mouse embryos. *Blood* 2000;95:1827–18.
35. Means RT Jr, Krantz SB. Inhibition of human erythroid colony-forming units by tumor necrosis factor requires beta interferon. *J Clin Invest*. 1993;91(2):416–9.
36. Tallack MR, Keys JR, Perkins AC. Erythroid Kruppel-like factor regulates the G1 cyclin dependent kinase inhibitor p18INK4c. *J Mol Biol* 2007;369(2):313–21.
37. Libani IV, et al. Decreased differentiation of erythroid cells exacerbates ineffective erythropoiesis in beta-thalassemia. *Blood* 2008;112(3):875–85.
38. Spring FA, et al. Intercellular adhesion molecule-4 binds alpha(4) beta(1) and alpha(V)-family integrins through novel integrin-binding mechanisms. *Blood* 2001;98(2):458–66.
39. Sadahira Y, Yoshino T, Monobe Y. Very late activation antigen 4-vascular cell adhesion molecule 1 interaction is involved in the formation of erythroblastic islands. *J Exp Med*. 1995;181(1):411–5.
40. Xue L, Galdass M, Gnanapragasam MN, Manwani D, Bieker JJ. Extrinsic and intrinsic control by EKLF (KLF1) within a specialized erythroid niche. *Development* 2014;41(11):2245–54.
41. Cocco C, Melis GV, Ferri GL. Embedding media for cryomicrotomy: an applicative reappraisal. *Appl Immunohistochem Mol Morphol* 2003;11:274–80.